DOI: 10.1002/ejoc.201000749

Full Structural Characterization of an Extracellular Polysaccharide Produced by the Freshwater Cyanobacterium *Oscillatoria planktothrix* FP1

Alba Silipo,*[a] Antonio Molinaro,[a] Monica Molteni,[b,c] Carlo Rossetti,[d] Michelangelo Parrilli,[a] and Rosa Lanzetta[a]

Keywords: Carbohydrates / Configuration determination / NMR spectroscopy / Structure elucidation / Environmental chemistry

Cyanobacteria, also known as blue-green algae or Cyanophyta, represent one of the oldest forms of life on Earth. The organisms exhibit a high degree of biological adaptation and comprise a large group of aquatic and photosynthetic oxygenic prokaryotes that obtain their energy through photosynthesis. Cyanobacterial extracellular polysaccharides are high-molecular-mass hetero-polysaccharides that are present on or released onto the cell surface and are characterized by high variability. In the present work we defined the structure of the extracellular polysaccharide produced by the freshwater cyanobacterium *Oscillatoria planktothrix* FP1. The structural determination, which was achieved by chemical, spectroscopic, and computational analyses, indicates a novel pentasaccharide repeating unit made up of glucose, mannose, and 2-deoxy-D-*ribo*-hexose, that has never previously been found in Nature. The elucidation of the structural and conformational features of the extracellular polysaccharide from *Oscillatoria planktothrix* is a first step toward understanding the biology of these important and interesting microorganisms.

Introduction

Cyanobacteria, also termed blue-green algae, constitute a large family of phylogenetically coherent photosynthetic bacteria that also include chloroplasts, representing one of the oldest forms of life on earth,[1–3] and estimated to have existed for approximately 3.5 million years. As the first organisms to use oxygenic photosynthesis, cyanobacteria were key players in the early evolution of life. They have a high degree of biological adaptation, inhabit all types of aquatic environment, and are known to occur in marine water, in which they are a significant component of the nitrogen cycle, in fresh and brackish water, lake sand, arid areas, and are an important component of phytoplankton. Moreover, the presence and detrimental action of microorganisms on monuments and the stonework of art has received considerable attention in the last few years. Cyanobacteria contribute to the maintenance of ecosystem health and are a source of biologically active industrial and pharmaceutical products, however, they also produce a variety of toxins, some of which are implicated in the pathogenesis of severe, chronic, and potentially life-threatening diseases in humans.

Cyanobacteria bear cell envelopes that resemble that of Gram-negative bacteria, consisting of an outer membrane located outside the cytoplasmic membrane and the peptidoglycan layer,[4,5] although structural differences can be highlighted. The peptidoglycan layer in cyanobacteria is considerably thicker than that of most Gram-negative bacteria and is complexed with specific polysaccharides. The lipopolysaccharides (LPS) of some cyanobacteria lack the typical components of the enterobacterial LPS;[4–6] it may contain only small amounts or be completely devoid of phosphate, but can also often lack heptose and Kdo (3-deoxy-D-*manno*-oct-2-ulosonic acid), the latter being always present in the LPS of Gram-negative bacteria. Frequently, cyanobacterial cells are covered by external surface layers such as S-layers and carbohydrate structures. In respect of carbohydrate structures, several cyanobacteria are able to synthesize and secrete extracellular polysaccharides,[7] which are usually associated with the outer surface of the bacterium and either covalently linked or loosely attached to the cell surface.[7,8] Such bacterial polysaccharides can, in fact, form an amorphous layer of extracellular polysaccharides (EPS) that are released onto the cell surface and surround the cell with no clear means of attachment, often forming a slime. In contrast, capsular polysaccharides are covalently linked to the cell surface of the bacteria through phospholipid mo-

[a] Dipartimento di Chimica Organica e Biochimica, Università di Napoli "Federico II", Complesso Universitario Monte S.Angelo, via Cintia 4, 80126 Napoli, Italy
Fax: +39-081-674393
E-mail: silipo@unina.it
[b] Bluegreen Biotech s. r. l., Milano, Italy
[c] Dipartimento Ambiente e Salute, Istituto di Ricerche Farmacologiche Mario Negri, Milano, Italy
[d] Dipartimento di Biotecnologie e Scienze Molecolari, Università degli Studi dell'Insubria, Varese, Italy

Supporting information for this article is available on the WWW under http://dx.doi.org/10.1002/ejoc.201000749.

lecules. Cyanobacterial polysaccharides can be homo- or hetero-polymeric and can also carry non-glycidic appendages such as phosphate, sulfate, lactate, acetate, and glycerol.[7] Often, they possess a significant level of hydrophobicity, due to the presence of acetyl groups, peptide moieties, and deoxysugars, which confer to the polysaccharide emulsifying properties and lead to some interesting rheological characteristics. Bacterial polysaccharides mediate direct interactions between the microorganism and its immediate environment and are involved in a number of biological processes; they also play a role in the virulence of many animal and plant pathogens. Furthermore, cyanobacterial polysaccharides act as protecting agents against dehydration due to their ability to entrap and accumulate water, creating a gelatinous layer around the cells that regulates water uptake and loss, thus stabilizing the cell during periods of desiccation, and protecting cells against phagocytosis, antibody recognition and lysis. They have also been implicated in several processes, such as metal chelation, due to the frequent presence of negatively charged sugars and substituents, or can even prevent direct contact with toxic heavy metals. Moreover, these polysaccharides can modify the rheological properties of water, act as thickening agents, and have the capacity to protect cyanobacterial cells from the harmful effects of UV irradiation; they also have a role in adhesion and locomotion and can protect cells from biomineralization processes. These polymers are of interest for potential biotechnological exploitation as, for example, viscosying or suspension agents in the food, cosmetic, and textile industries, for their capacity to modify the flow properties of water, and as metal ion sequestrating agents in the pharmaceutical industry.[7]

In the present work, we have defined for the first time the structure and the solution conformation of the exopolysaccharide produced by the freshwater cyanobacterium *Oscillatoria planktothrix* FP1. This strain produces a polymer with a branched pentasaccharide repeating unit that is characterized by the presence of glucose, mannose, and 2-deoxy-D-*ribo*-hexose. The latter, to the best of our knowledge, is the first such naturally occurring example of its kind found in Nature. Due to the lack of reference compounds, its absolute configuration was determined by 2D NMR spectroscopy; the findings were supported by molecular mechanical and dynamic calculations[9,10,11] and by the application of Klyne's rule.[12]

Results and Discussion

Chemical Analysis

The compositional analysis of the isolated exopolysaccharide from *Oscillatoria planktothrix* FP1 (Exo-Cy) showed the presence of mannose, glucose, and an unidentifiable 2-deoxy-hexose. The absolute configurations of both glucose and mannose were determined to be D by GLC of the acetylated (*S*)-2-octyl glycosides and comparison with authentic standards. Methylation analysis showed the presence of 2,4-substituted-Man*p*, 4-substituted-Glc*p*, terminal glucose, and 4,5-substituted-2-deoxy-hexose.

Structural Elucidation of Acid Hydrolyzed Product (OS)

Due to the insolubility of the exopolysaccharide in aqueous solvent and considering the presence of an acid-labile deoxysugar, it was depolymerized under mild acid hydrolysis and purified by gel-permeation chromatography to give the oligosaccharide (**OS**) product. The monosaccharide analysis of **OS** gave the same results as for intact polymer, meaning that the compositional integrity of the sugar remained unchanged during chemical treatment. The oligosaccharide product was characterized by full 2D NMR analysis; the ^{1}H NMR spectrum of the OS product is shown in Figure 1 (a). A combination of homo- and hetero-nuclear 2D NMR experiments (DQF-COSY, TOCSY, T-ROESY, ^{1}H,^{13}C-HSQC, ^{1}H,^{13}C-HMBC) were conducted to assign all the spin systems and to define the saccharidic sequence. Complete assignment of the sugar residues was accomplished by attributing the proton resonances from the DQF-COSY and TOCSY spectra, and by subsequently

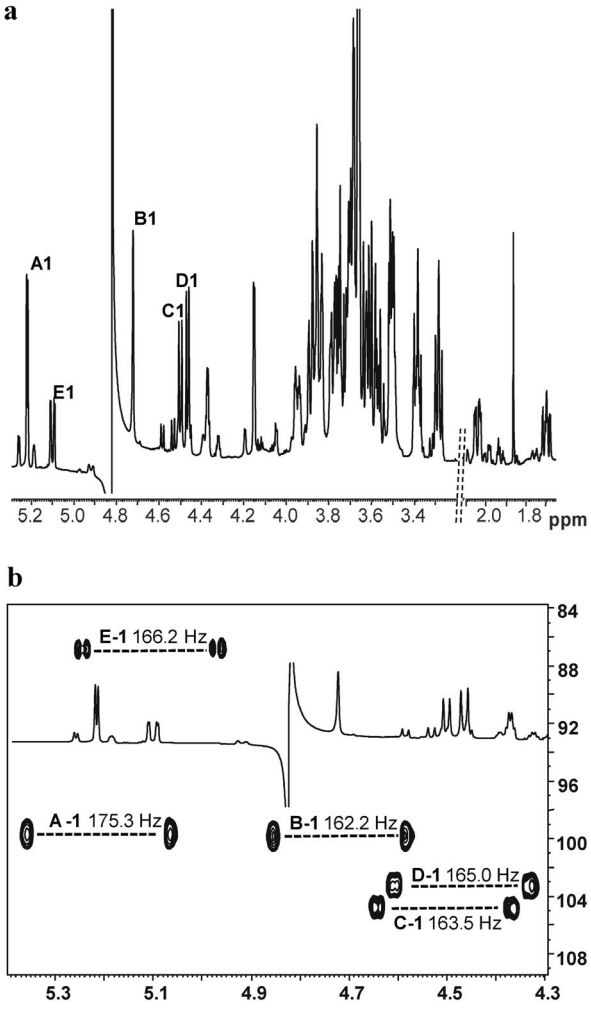

Figure 1. (a) ^{1}H NMR spectrum (600 MHz) of the oligosaccharide (**OS**) derived from acid treatment of the exopolysaccharide of *Oscillatoria planktothrix* FP1. Key NMR signals are as indicated in Table 1; (b) Expansion of the anomeric region of the ^{1}H NMR spectrum and of the F2-coupled HSQC spectra in which the diagnostic heteronuclear anomeric constants are shown.

correlating each proton to its related carbon atom by reference to the HSQC spectrum. The anomeric configuration of each monosaccharide unit was assigned on the basis of the $^3J_{H\text{-}1,H\text{-}2}$ coupling constant values obtained from the DQF-COSY experiment, the $^1J_{C1,H1}$ constants (Figure 1, b)[13] derived from *F*2-coupled HSQC measurements, and were confirmed by the intra-residual NOE contacts observed in the T-ROESY spectrum (Figure 2, a). The values of the vicinal $^3J_{H,H}$ ring coupling constants allowed identification of the relative configuration of each sugar. The absence of carbon resonances above δ = 80 ppm testified to the absence of sugar residues in the furanose form.

Residues **A**, **C**, and **D** were all identified as *gluco*-configured sugar residues, as indicated by the large $^3J_{H,H}$ ring coupling constants and by the chemical shift values, which are in agreement with the *gluco*-configuration of pyranose rings in a $^4C_1$ conformation (Table 1). In particular, residue **A** (H-1 at δ = 5.21 ppm Table 1) was recognized as α-glucose; the α-configuration was assigned by the $^1J_{C1,H1}$ and $^3J_{H1,H2}$ values (175.3 and 3.85 Hz, respectively), and confirmed by the intraresidual NOE contact between H-1 and H-2 and by the H-5/C-5 chemical shift values. Spin systems **C** and **D** (H-1 at δ = 4.51 and 4.47 ppm, respectively) were both identified as β-glucose residues; both $^1J_{C1,H1}$ and $^3J_{H1,H2}$ values, together with the NOE contacts of H-1 with H-3 and H-5, were diagnostic of β-anomeric configurations.

Spin system **B** (Table 1) was identified as a β-mannose residue; the *manno* configuration was indicated by the low $^3J_{H\text{-}1,H\text{-}2}$ and $^3J_{H\text{-}2,H\text{-}3}$ ring coupling constants (less than 1 Hz), and the β-anomeric configuration was inferred by the heteronuclear $^1J_{C1,H1}$ value (162.2 Hz) together with the strong intra-residual NOE contacts of H-1 with H-3 and H5, which is diagnostic of the β-anomeric configuration (Figure 2).

Spin system **E** (Table 1, H-1 at δ = 5.11 ppm) was identified as a β-2-deoxy-*ribo*-hexopyranose residue (β-2-deoxy-*allo*-pyranose or β-2-deoxy-*altro*-pyranose, henceforth abbreviated as β-2d-All*p*). The deoxy position was located,

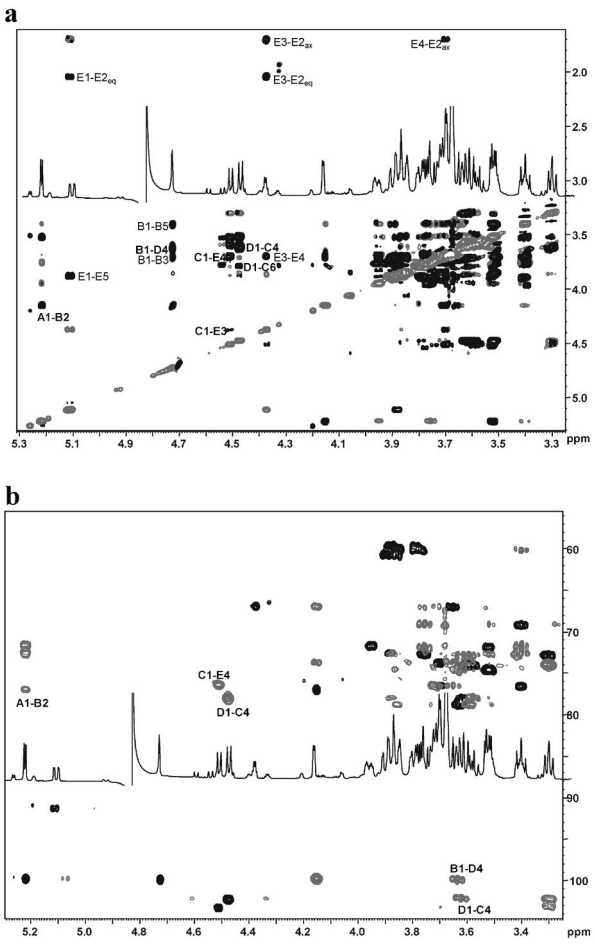

Figure 2. (a) Expansion of the TOCSY (grey) and T-ROESY (black) spectra in which the key inter-residual NOE contacts are indicated (printed in **bold**); intra-residual NOE contacts diagnostic of the configuration of residues **B** and **F** were also highlighted (in plain text); (b) Expansion of the HSQC (grey) and HMBC (black) spectra in which the key inter-residual scalar long-range correlations are indicated.

Table 1. ^{1}H and ^{13}C NMR chemical shifts (δ, ppm), and $^1J_{C,H}$ and $J_{H,H}$ coupling constants for pentasaccharide **OS** derived from acid hydrolysis. All sugar residues are in D-configuration and in pyranose form; *red* stands for reducing.

Unit	1	2	3	4	5	6
A	5.21 (d)	3.52	3.76	3.40	3.94	3.76/3.69
t-α-Glc	99.5	71.9	72.5	69.2	71.6	60.3
	$^1J_{C,H}$ = 175.3, $^3J_{H1,H2}$ = 3.85 Hz					
B	4.73 (br. s)	4.14	3.70	3.66	3.39	3.89/3.71
2-β-Man	99.8	76.9	73.7	67.0	76.5	60.7
	$^1J_{C,H}$ = 162.2, $^3J_{H1,H2}$< 1 Hz					
C	4.51 (d)	3.29	3.57	3.61	3.52	3.79/3.87
4-β-Glc	103.2	72.7	74.1	78.0	74.5	59.6
	$^1J_{C,H}$ = 163.5, $^3J_{H1,H2}$ = 8.01 Hz					
D	4.47 (d)	3.30	3.60	3.62	3.52	3.71/3.84
4-β-Glc	102.2	72.7	74.3	78.8	74.5	60.0
	$^1J_{C,H}$ = 165.0, $^3J_{H1,H2}$ = 7.88 Hz					
E	5.11 (dd)	1.69/2.02	4.38	3.70	3.86	3.85/3.72
red-4-β-2d-All	91.4	37.4	66.6	76.3	72.6	60.9
	$^1J_{C,H}$ = 166.2, $^3J_{H1,H2ax}$ = 9.9, $^3J_{H1,H2eq}$ = 1.95 Hz	$^2J_{H2ax,H2eq}$ = 12.1 Hz	$^3J_{H3,H2a}$ = 2.8, $^3J_{H3,H2b}$ = 3.5 Hz	$^3J_{H3,H4}$ <1 Hz		

in accordance with the chemical analysis, at the 2-position through scalar correlation of the H-1 anomeric proton with the diastereotopic H-2 axial/equatorial methylene protons resonating at δ = 1.69/2.02 ppm. The β-anomeric orientation was assigned by measuring the $^1J_{C1,H1}$ and $^3J_{H\text{-}1,H\text{-}2ax}$ coupling constants (Table 1, J = 166.2 and 9.9 Hz) and by noting the intra-residual NOE contact between H-1 and H-5 (Figure 2, a). Mild acid treatment revealed residue **E** to be the free reducing end in the **OS**, due to the acid lability of the 2-deoxysugar. The anomeric equilibrium was displaced toward the β-anomer in a β:α ratio of >80:20 (the α-anomer resonated at δ = 5.59/100.0 ppm). Both ring coupling constants and chemical shift values were in agreement with the existence of a pyranose ring in chair conformation. The *ribo*-hexose configuration was established from the $^3J_{H\text{-}3,H\text{-}2ax/eq}$ (ca. 3 Hz) and $^3J_{H\text{-}3,H\text{-}4}$ values (less than 1 Hz, Table 1), which is diagnostic of an axial orientation of O-3, and further confirmed by the absence of an NOE contact between H-1 and H-3, which is always found as an intense signal in the NOESY spectra of β-configured sugar residues when these protons are oriented in a *syn*-diaxial manner. Moreover, the NOE correlation between H-2 and H-4 testified to their *syn*-diaxial orientation, thus confirming the *ribo*-hexose relative configuration (Figure 2, b).

An analysis of the scalar and dipolar inter-residual correlations in the 2D NMR spectra (Figure 2, parts a and b) allowed the identification of a pentasaccharide structure. The downfield shift of the carbon resonances identified the glycosylated positions: the O-2 of residue **B**, and the O-4 of residues **C**, **D**, and **E**, whereas residue **A** was a nonreducing terminal sugar, in full agreement with the methylation analysis. The inter-residual NOE contacts (Figure 2, a) and the long-range correlations present in the HMBC spectrum (Figure 2, b) yielded the oligosaccharide sequence. The β-mannose **B** was glycosilated at O-2 by α-glucose **A**, as suggested by the NOE contact between H-2 of **B** (δ = 4.14 ppm) and H-1 of **A** (δ = 5.21 ppm) (Figure 2, a). Spin system **B** was, in turn, positioned at O-4 of the β-glucose **D**, as attested to by the NOE contact between H-1 of **B** and H-4 of **D**. The β-(1→4) linkage between the two β-glucose residues **C** and **D** was established by the NOE contact H-1 of **D** with H-4 of **C**. Finally, residue **C** was located at O-4 of the β-2-deoxy-*ribo*-hexose **E**, as shown by the NOE contact between H-1 of **C** and H-4 of **E** (Figure 2, a). The sequence of this repeating unit was confirmed by the long-range scalar correlations found in the HMBC spectrum (Figure 2, a). Thus, all data were in agreement with the pentasaccharide structure shown below (*red* stands for reducing).

A **B** **D** **C** **E**
α-D-Glc-(1→2)-β-D-Man-(1→4)-β-D-Glc-(1→4)-β-D-Glc-(1→4)-β-2d-All-*red*

To determine the absolute configuration of the 2-deoxy-*ribo*-hexose unit, we used both a computational approach [9,10,11] and the Klyne rule.[12,14] These methods overcame the problems associated with the lack of monosaccharide references and the difficulties associated with its isolation. Lipkind et al.[9] exploited the relative intensities of the inter-residual NOE effects by analyzing the structural and stereochemical factors determining the conformation of the glycosidic linkages; data showed that the main structural factors determining the NOE and the preferred conformation in disaccharide units were the configuration of the glycosidic linkage, the nature of the sugar, the position of glycosidation, and the absolute configuration of the constituent residues. To gain an insight into the absolute configuration of the 2-deoxy-*ribo*-hexose unit, a protocol based on a comparison of the key inter-proton distances experimentally obtained from the NOE data and those predicted for different models taking into account the two possible absolute configurations of residue **E** (L and D) has been applied. The application of this protocol is possible because the absolute configuration of the other sugar residue was known.

As a starting point, two distinct disaccharide entities, namely **C**-4$\mathbf{E_D}$ and **C**-4$\mathbf{E_L}$, were constructed with glucose **C** in the D-configuration and the 2-deoxy-*ribo*-hexose **E** drawn with both D- and L-configuration (Figure 3); the models were subjected to extensive calculations using the MM3* force field to build potential energy surfaces for both disaccharides with relative orientations defined by Φ and Ψ torsion angles around the glycosidic linkage. The resulting adiabatic energy maps, indicating both global and local minima, are reported in Figure 3 (a). Molecular mechanics provided an estimation of the conformational regions that are energetically accessible and predicted the existence of slightly different minima for the two glycosidic linkages: for the D,D-disaccharide, the global minimum was located at Φ/Ψ = 51.0/–15, whereas for D,L-disaccharide the minima were located at Φ/Ψ = 52/16 (Figure 3, a). Ensemble average inter-proton distances for each disaccharide entity were extracted from the molecular mechanical calculations and translated into predicted NOEs by a full-matrix relaxation approach; NOEs were then compared with those experimentally collected to establish the reliability of the simula-

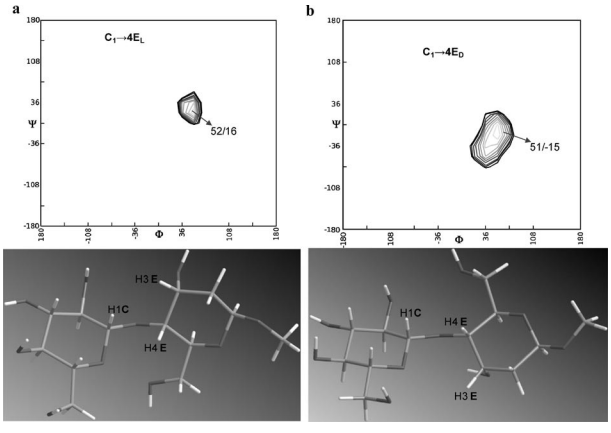

Figure 3. (a and b, top) Relaxed energy maps for the disaccharide fragments $\mathbf{C_1 \rightarrow 4E}$, which differ in the absolute configuration of residue **E**. The position of the global minima in the maps are indicated; (a and b, bottom) View of representative structures of $\mathbf{C_1 \rightarrow 4E}$ disaccharides differing in the absolute configuration of **E**; the key protons for the definition of the absolute configuration of **E** in the oligosaccharide are indicated (see text).

Table 2. Experimental (from T-ROESY experiments) and calculated (from MD calculations) key inter-proton distances for the pentasaccharide obtained from acid hydrolysis. All data refer to the β-conformer, which was present in amounts greater than 80%. The experimental values were obtained as described in the experimental part by applying the isolated spin pair approximation.

	Experimental [Å]	NOE observed	Calculated D,D- disaccharide C-4E [Å]	Calculated D,D-pentasaccharide [Å]	Calculated D,L- disaccharide C-4E [Å]	Calculated D,L-pentasaccharide [Å]
C1–E3	3.23	medium	3.45	3.22	2.53	2.50
C1–E4	2.31	strong	2.39	2.39	2.60	2.57
C1–E5	n.d.	absent	4.38	4.46	4.55	4.68

tion data. The experimental values were in good agreement with the conformation adopted by the disaccharides (not shown). The conformational space available to the tetrasaccharide was next investigated by MD simulations. Computational models of the two disaccharides and the whole pentasaccharide were generated by using the energy minima for each glycosidic junction from the disaccharide energy maps obtained with the MM approach. The initial structures were extensively minimized and the trajectory coordinates were sampled every picosecond; 4000 simulations were performed in a GB/SA water solvation model as implemented in MacroModel (MMOD). The computational models obtained from the MD were then compared to the experimental results. Ensemble average inter-proton distances for each molecule were extracted from dynamic simulations and translated into NOE contacts according to a full-matrix relaxation approach. The corresponding average distances obtained from the simulation from $<r^{-6}>$ values and predicted for both disaccharides and pentasaccharides built with residue **E** in D- and L-configurations were compared to those collected experimentally (Table 2 and Figure 3). A comparison of the simulated NOEs with those obtained for the authentic sample and the corresponding distances (Table 2) allowed the absolute D-stereochemistry of residue **E** to be established; in fact, an excellent agreement was observed between the calculated and the experimental data.

The key NOE correlations considered for the definition of the absolute configuration of **E** were those between H-1 of **C** and H-3 of **E** (medium) and H-4 of **E** (strong). In fact, the strong NOE correlation between H-1 of **C** with H-4 of **E** and the medium NOE correlation with H-3 of **E** would only be expected when unit **E** had D-configuration (see Table 2 and Figures 2, 3 (a), and 4); the corresponding derived inter-proton distances were in excellent agreement with the experimentally observed values. When the L-configuration is considered, two strong NOE correlations between H-1 of **C** and H-3 and H-4 of **E** would be expected and, as a consequence, the calculated inter-proton distances differed significantly from the experimentally observed values (Table 2). An analysis of the computational models of D,D- and D,L-disaccharides (Figure 3, b) and pentasaccharides confirmed this hypothesis. Figure 4 shows a snapshot of a representative conformer of the pentasaccharide with the 2-deoxy-*ribo*-hexose in the D-configuration.

To corroborate this hypothesis, the absolute configuration of residue **E** was confirmed by consideration of the molecular rotation values of the oligosaccharide by using

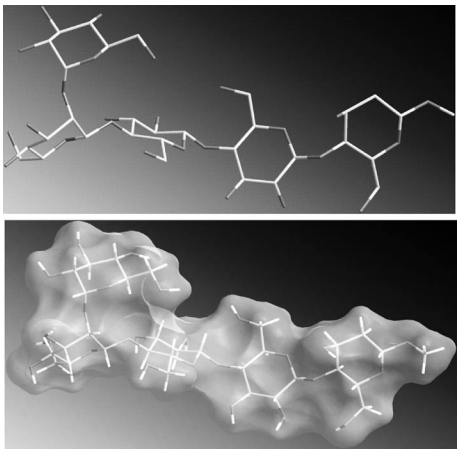

Figure 4. View of a representative structure and the Connelly surface of the oligosaccharide **OS** α-D-Glc-(1→2)-β-D-Man-(1→4)-β-D-Glc-(1→4)-β-D-Glc-(1→4)-β-D-2d-All.

Klyne's rule;[12,14] the application of which firmly indicated a D-configuration for **E** (Table 3). In fact, the two alternative combinations (obtained by supposing the presence of residue **E** with D- or L-configuration in the pentasaccharide chain) gave calculated $[M]_D$ values of –22.1° for the L-configuration of **E** and +166.7° for the D-configuration of **E** – both of which differ considerably from the observed value of 192.2°.

Table 3. Observed and calculated $[M]_D$ values for the **OS** when the alternative contribution of 2-deoxy-ribohexose enantiomers are considered.

$[M]_D$ Observed	+192.2
$[M]_D$ Calculated **D-2dAll**	+166.7[a]
$[M]_D$ Calculated **L-2dAll**	–22.1[a]

[a] The calculated $[M]_D$ values were obtained by addition of those of the methyl-glycosides of each residue with known configuration of the pentasaccharide to the $[M]_D$ of the alternative 2d-All enantiomers ($[\alpha]_D$ values from *Dictionary of carbohydrates* (Ed.: Peter M. Collins), Chapman & Hall, 1998).

Partial Structural Elucidation of the Smith Degradation Product (OS_{Smith})

To complete the structure of the exopolysaccharide produced by *Oscillatoria planktothrix*, the linkage of the acid-labile 2-deoxy-*ribo*-hexose, and its anomeric configuration

Table 4. Partial ^{1}H and ^{13}C NMR assignments (δ, ppm) of the polysaccharide derived from the Smith degradation. All sugar residues are in the D-configuration.

Unit	1	2	3	4	5	6
B′	4.81	4.30	3.82	3.86	3.55	3.72/3.85
2-β-Man	99.8 ($^1J_{C,H}$ = 164.2 Hz)	76.9	71.9	76.3	75.0	60.0
E′	5.00	2.19/1.83	4.48	3.81	3.99	3.78
4-β-2d-All	98.5 ($^1J_{C,H}$ = 167.6 Hz)	36.2	66.7	76.6	72.5	60.7
A′	5.35	3.605				
t-Glc	99.5	62.1				
C′/D′	5.11	3.79/3.68	3.78/3.76	4.10	3.72	3.70
4-Glc	104.2	61.02	60.7	78.7	74.0	60.4

in the polysaccharide remained to be established. The first step was to generate a polymer with good solubility so that it could be examined by using NMR spectroscopy. Given the absence of any vicinal diol functionality in both mannose and deoxy-*ribo*-hexose residues, we decided to carry out a Smith reaction[15] (periodate degradation) to leave these sugars unaffected and to degrade the other residues; to avoid acid treatment, which would have affected the labile glycosidic linkage(s) of the deoxy-sugar, we avoided the usual second step of acid hydrolysis and studied the polysaccharide derived from the Smith oxidation and the subsequent reduction of the produced carbonyl groups. Actually, the polysaccharide was water-soluble.

Methylation analysis of the sample indicated the presence of only two monosaccharide derivatives: 2,4-substituted Mannose and terminal 2-deoxy-*ribo*-hexose. The polysaccharide was examined by NMR spectroscopy (the ^{1}H NMR spectrum is shown in Figure S1a in the Supporting Information) and Table 4 reports the NMR proton assignments. The anomeric configuration of the monosaccharide unit was assigned on the basis of $^1J_{C1,H1}$ coupling constants,[13] which were established from F2-coupled HSQC experiments. Spin system **B′** (Table 4) was identified as the β-mannose residue; the heteronuclear $^1J_{C1,H1}$ value (164.2 Hz) together with the NOE contacts of H-1 with H-3 and H-5 was diagnostic of the β-anomeric configuration.

Spin systems **E′** (Table 4, H-1 at δ = 5.11 ppm), was identified as the β-2-deoxy-*ribo*-hexose residue (β-2d-All*p*). The β-anomeric orientation was assigned on the basis of the $^1J_{C1,H1}$ coupling constants (Table 4, 167.6 Hz) and on the intra-residual NOE contact between H-1 with H-5, which confirms that this unit was present in the exopolysaccharide with β-configuration. Analysis of the dipolar inter-residual correlations in the 2D NMR spectra (Figure S1b in the Supporting Information) allowed the link between the β-mannose and the β-2-deoxy-*ribo*-hexose to be identified. The downfield shift of the carbon resonances identified the glycosylated positions of residues O-2 and O-4 of **B′**, and O-4 of **E** (only those unaffected by the Smith degradation).

Thus, structural data derived from acid treatment and the Smith degradation were in agreement with the pentasaccharide structure shown below, which represents the repeating unit of the exopolysaccharide produced by the cyanobacterium *Oscillatoria planktothrix* FP1.

α-D-Glc
↓
2
[→4)-β-D-Man-(1→4)-β-D-Glc-(1→4)-β-D-Glc-(1→4)-β-D-2d-All-(1→]$_n$

Conclusions

The extracellular polysaccharide produced by the freshwater cyanobacterium *Oscillatoria planktothrix* FP1 consists of a novel pentasaccharide repeating unit made up of glucose, mannose, and 2-deoxy-D-*ribo*-hexose, this latter unit has never previously found in Nature.

The absolute configuration of this sugar was defined by using a molecular mechanical approach and supported by an application of Klyne's rule. Knowledge of the structural and conformational features of this repeating unit will contribute to an understanding of its biological role.

Experimental Section

Bacterial Strain and Growth Conditions: Cultures from cyanobacterium *Oscillatoria Planktothrix* FP1 were grown in 1 L flasks containing 600 mL of BG11 freshwater medium (Sigma–Aldrich) at 27 °C under constant irradiance of cool white light at an intensity of 20 μmol photon m^{-2} s^{-1}.[16]

Extracellular Polysaccharide (EPS) Isolation: EPSs were isolated as described by Moreno et al.[17] with some modification. Cell cultures were collected at the stationary phase of growth by centrifugation at 4000 *g* for 15 min and then incubated in distilled water at 50 °C for 20 min. Separation of the EPS from the cells was performed by centrifugation at 8000 *g* for 15 min. EPS in the supernatants was then precipitated by addition of 10 mM sodium acetate and two volumes of cold acetone, and recovered by centrifugation at 4000 *g* for 15 min at 4 °C. Pellets were washed with 70% ethanol and incubated overnight at 37 °C with 100 μg/mL proteinase K in 25 mM TRIS (pH 8.5). EPS was then recovered by centrifugation at 4000 *g* for 15 min. and employed for analytical work.

Chemical Analysis: Determination of sugar residues and their absolute configuration through GC-MS analyses, were all carried out as described.[18–19] Monosaccharides were identified as acetylated *O*-methyl glycoside derivatives. After methanolysis (2 M HCl/MeOH, 85 °C, 2–18 h) and acetylation with acetic anhydride in pyridine (85 °C, 30 min), the sample was analyzed by GC-MS. The absolute configuration of the sugar residues was determined by GC-MS analysis of the acetylated *O*-(+)-oct-2-yl glycoside derivatives (octanolysis at 85 °C, 18 h; acetylation with acetic anhydride in pyridine, 85 °C, 40 min) and comparison to authentic standards.

Linkage analysis was carried out by methylation of the saccharide chain as described:[20] the sample was methylated with iodomethane, hydrolyzed with 2 M trifluoroacetic acid (100 °C, 2 h), the carbonyl was reduced with $NaBD_4$, acetylated with acetic anhydride and pyridine, and analyzed by GC-MS.

Smith Degradation: An aliquot of the polysaccharide (15 mg) was modified by periodate oxidation and successive reduction. The sample was dissolved in water (1 mL), to which 0.1 M $NaIO_4$ solution (3 mL) was added, and the mixture was kept at 4 °C for 100 h. The reaction was quenched by adding pure ethylene glycol (10 μL), neutralized with 0.5 M NaOH, and then reduced with $NaBH_4$, followed by extensive dialysis.

NMR Analysis: For structural assignments, 1D and 2D ^{1}H NMR spectra were recorded in D_2O at 300 K, at pD 7, with a Bruker 600 DRX instrument equipped with a cryo probe; spectra were calibrated with internal acetone [δ_H = 2.225 ppm, δ_C = 31.45 ppm]. ROESY and NOESY experiments were recorded using data sets ($t_1 \times t_2$) of 4096 × 256 points with mixing times between 100 and 400 ms. Double quantum-filtered phase-sensitive COSY experiments were performed using data sets of 4096 × 256 points. TOCSY experiments were performed with spinlock times of 100 ms, using data sets ($t_1 \times t_2$) of 4096 × 256 points. In all homonuclear experiments the data matrix was zero-filled in both dimensions to give a matrix of 4K × 2K points and was resolution-enhanced in both dimensions by a cosine-bell function before Fourier transformation. Coupling constants were determined by 2D phase-sensitive DQF-COSY.[21–22] HSQC and HMBC experiments were measured in the ^{1}H-detected mode via single quantum coherence with proton decoupling in the ^{13}C domain, using data sets of 2048 × 256 points. Experiments were carried out in the phase-sensitive mode.[23] A 60 ms delay was used for the evolution of long-range connectivities in the HMBC experiment. In all heteronuclear experiments the data matrix was extended to 2048 × 1024 points using forward linear prediction extrapolation.

1D ^{1}H NMR experiments for diffusion measurements on the polysaccharide from Smith degradation were performed using a stimulated echo sequence with bipolar gradient pulses and one spoil gradient (stebpgp1s1d); 128 scans were collected, with a gradient duration δ from 4 to 16 ms and an echo delay (diffusion time) Δ kept constant at 100 ms. Following the optimization of DOSY parameters by 1D experiments, diffusion filtered 2D TOCSY sequence (ledbpgpml2s2d) was used with diffusion filter using stimulated echo and LED (longitudinal eddy current delay); bipolar gradient pulses for diffusion and two spoil gradients were used; the mixing time length for the TOCSY spin lock was set to 100 ms.

Conformational Studies: Molecular mechanics calculations were performed using the MM3* force field as included in MacroModel 8.0. A dielectric constant of 80 was used. For each disaccharide structure, both Φ and Ψ were varied incrementally using a grid step of 18°, each (Φ,Ψ) point of the map was optimized using 2000 P. R. conjugate gradients. The molecular dynamic simulations were run by using the MM3* force field; bulk water solvation was simulated by using the MacroModel generalized Born GB/SA continuum solvent model. All simulations were performed at 300 K, structures were initially subjected to an equilibration time of 300 ps, then a 10000 ps molecular dynamic simulation was performed with a dynamic time-step of 1.5 fs, a bath constant t of 0.2 ps and the SHAKE protocol to the hydrogen bonds. Trajectory coordinates were sampled every 2 ps, and a total of 5000 structures were collected for every simulation.[24–26] Ensemble average-interproton distances were calculated using the NOEPROM program[27] by applying the isolated spin pair approximation as described.[28] Coordinate extractions were performed with the program SuperMap, supplied with the NOEPROM package, and data were visualized with ORIGIN software. Solvent-accessible surfaces were calculated with the Surface utility of Macromodel and with Molecular Surface displays of Chem3D package.

Supporting Information (see also the footnote on the first page of this article): Figures S1a and S1b.

[1] R. Y. Stanier, G. Cohen-Bazire, *Annu. Rev. Microbiol.* **1977**, *31*, 225–274.
[2] M. A. Labine, G. Y. Minuk, *Can. J. Physiol. Pharmacol.* **2009**, *87*, 773–788.
[3] A. Macagno, M. Molteni, A. Rinaldi, F. Bertoni, A. Lanzavecchia, C. Rossetti, F. Sallusto, *J. Exp. Med.* **2006**, *203*, 1481–1492.
[4] E. Hoiczyk, A. Hansel, *J. Bacteriol.* **2000**, *182*, 1191–1199.
[5] E. Flores, A. Herrero, *Nat. Rev. Microbiol.* **2010**, *8*, 39–50.
[6] D. S. Snyder, B. Brahamsha, P. Azadi, B. Palenik, *J. Bacteriol.* **2009**, *191*, 5499–5509.
[7] S. Pereira, A. Zille, E. Micheletti, P. Moradas-Ferreira, R. De Philippis, P. Tamagnini, *FEMS Microbiol. Rev.* **2009**, *33*, 917–941, and references therein.
[8] I. S. Roberts, *Annu. Rev. Microbiol.* **1996**, *50*, 285–315.
[9] G. M. Lipkind, A. S. Shashkov, S. S. Mamyan, N. K. Kochetkov, *Carbohydr. Res.* **1988**, *181*, 1–12.
[10] J. Jimenez-Barbero, C. de Castro, A. Evidente, A. Molinaro, M. Parrilli, G. Surico, *Eur. J. Org. Chem.* **2002**, 1770–1775.
[11] C. de Castro, A. Molinaro, A. Wallace, W. D. Grant, M. Parrilli, *Eur. J. Org. Chem.* **2003**, 1029–1034.
[12] W. Klyne, *Biochem. J.* **1950**, *47*, 4.
[13] K. Bock, C. Pedersen, *J. Chem. Soc. Perkin Trans. 2* **1974**, *2*293–297.
[14] M. Adinolfi, G. Barone, R. Lanzetta, G. Laonigro, L. Mangoni, M. Parrilli, *Can. J. Chem.* **1984**, *62*, 1223–1226.
[15] F. Smith, R. Montgomery, *Methods Biochem. Anal.* **1956**, *3*, 153–212.
[16] M. Prati, M. Molteni, F. Pomati, C. Rossetti, G. Bernardini, *Toxicon* **2002**, *40*, 267–272.
[17] J. Moreno, M. A. Vargas, J. M. Madiedo, J. Munoz, J. Rivas, G. M. Guerrero, *Biotechnol. Bioeng.* **2000**, *67*, 283–290.
[18] K. Leontein, J. Lönngren, *Methods Carbohydr. Chem.* **1978**, *62*, 359–362.
[19] A. Molinaro, C. De Castro, R. Lanzetta, A. Evidente, M. Parrilli, O. Holst, *J. Biol. Chem.* **2002**, *277*, 10058–10063.
[20] S. Hakomori, *J. Biochem. (Tokyo)* **1964**, *55*, 205–208.
[21] U. Piantini, O. W. Sørensen, R. R. Ernst, *J. Am. Chem. Soc.* **1982**, *104*, 6800–6801.
[22] M. Rance, O. W. Sørensen, G. Bodenhausen, G. Wagner, R. R. Ernst, K. Wüthrich, *Biochem. Biophys. Res. Commun.* **1983**, *117*, 479–485.
[23] D. J. States, R. A. Haberkorn, D. J. Ruben, *J. Magn. Reson.* **1982**, *48*, 286–292.
[24] S. Mari, I. Sánchez-Medina, J. Jimenez-Barbero, A. Bernardi, *Carbohydr. Res.* **2007**, *342*, 1859–1868.
[25] J. L. Asensio, F. J. Canada, X. Cheng, N. Khan, D. R. Mootoo, J. Jimenez-Barbero, *Chem. Eur. J.* **2000**, *6*, 1035–1041.
[26] A. Bernardi, D. Potenza, A. M. Capelli, A. Garcia-Herrero, F. J. Canada, J. Jimenez-Barbero, *Chem. Eur. J.* **2002**, *8*, 4598–4612.
[27] J. L. Asensio, J. Jiménez-Barbero, *Biopolymers* **1995**, *35*, 55–75.
[28] F. Corzana, I. Cuesta, F. Freire, J. Revuelta, A. Bastida, J. Jiménez-Barbero, J. L. Asensio, *J. Am. Chem. Soc.* **2007**, *129*, 2849–2865.

Received: May 25, 2010
Published Online: August 24, 2010

